Journal of Fluorine Chemistry 131 (2010) 1025–1031

Contents lists available at ScienceDirect

Journal of Fluorine Chemistry

journal homepage: www.elsevier.com/locate/fluor

P–C bond formation via P–H addition of a fluoroaryl phosphinic acid to ketones

Andreas Orthaber [a], Jörg H. Albering [b], Ferdinand Belaj [a], Rudolf Pietschnig [a,*]

[a] Department of Chemistry, Inorganic Section, University of Graz, Schubertstr. 1, 8010 Graz, Austria
[b] Institute of Chemistry and Technology of Materials, Graz University of Technology, Stremayrg. 16, 8010 Graz, Austria

ARTICLE INFO

Article history:
Received 18 May 2010
Received in revised form 9 July 2010
Accepted 18 July 2010
Available online 23 July 2010

Keywords:
Phosphorus
Tautomerism
Hydrogen bonds
Ab initio calculations
Fluorinated ligands

ABSTRACT

The synthesis, structure and reactivity of the fluoroaryl phosphinic acid HF_4C_6–P(O)HOH is reported and compared to a sterically comparable yet non-fluorinated analog with similar size. The fluoroaryl phosphinic acid undergoes reversible P–H addition to the carbonyl functionality of ketones under formation of a P–C bond which is retained in the resulting α-hydroxy phosphinic acid. The latter shows an extended 2D hydrogen bonded network in the solid state.

1. Introduction

Phosphinic acids are relevant for many fields of chemistry [1], biology [2] and medicinal chemistry [3]. On the other side, also phosphorus compounds with electron withdrawing moieties attracted considerable attention in the last decade. Electron withdrawing groups are known to influence electronic and optical properties of the phosphorus containing compounds besides their reactivity [4–7]. It has been demonstrated that the phosphinic acid $(CF_3)_2POH$ is the prevalent tautomeric structure over $(CF_3)_2P(=O)H$, which is in sharp contrast to other known phosphinic acids [8,9]. Also C_2F_5 substitution leads to a similar behavior [10]. By using 1,3 bis(trifluoro)methyl substituted aryl rings Hoge and co-workers showed that the corresponding phosphinic anhydrides can be stabilized over the tautomeric diphosphane monoxides which was attributed to the electronic nature of the fluorinated groups [11]. In the last years the synthesis of fluorinated phosphanes aiming at phosphano-borane based "frustrated" Lewis acid/base pairs has flourished enormously looking at applications as e.g. hydrogen activation and storage [12,13]. The perfluorinated phosphinic acid $(C_6F_5)_2P(=O)H$ forms an adduct with acetone in solution, which is however not retained in the solid state owing to its alleged kinetic instability [14]. By increasing the Lewis acidity of the carbonyl component the adduct formation becomes irreversible as is evidenced on going from acetone to benzaldehyde [14]. The resulting α-hydroxy phosphinic acids had been previously synthesized using alternative pathways [15–19]. For a non-fluorinated α-hydroxy phosphinic acid obtained by the latter route the isolation and characterization with X-ray diffraction of a single enantiomer (S) could be achieved [20]. Applications of this class of compounds range from flame retardants [21] to asymmetric synthesis [22] and neutral amino peptidase (NAPN) inhibitors [23].

We investigated the P–H addition of a phosphinic acid to acetone where the partially fluorinated substituent (HF_4C_6–) carries a single hydrogen atom as spectator unit for spectroscopic purposes. A comparison with the non-fluorinated mesityl phosphinic acids shows the influence of the electron withdrawing substituent on the phosphinic acid, while the steric demand of the fluorine groups should be only slightly smaller than that of the methyl groups [24,25]. For the partially fluorinated phosphinic acid we found a reversible addition equilibrium with acetone forming the corresponding α-hydroxy phosphinic acid. Surprisingly the latter is also stable in the solid phase, unlike its previously reported perfluorinated counterpart.

2. Results and discussion

The partially fluorinated substituent 2,3,5,6-tetrafluorophenyl (HF_4C_6–) turned out to be useful to track reactions employing the single hydrogen atom as a spectroscopic probe [26]. The corresponding dichlorophosphane **1a** which was recently published [26] should be a suitable precursor for the synthesis of phosphinic acid **2a**. For HF_4C_6-compounds the electronic and steric situation should be very similar to their C_6F_5 substituted analogs. On the other hand for the corresponding mesityl (Mes = 2,4,6-

* Corresponding author. Tel.: +43 316 380 5287; fax: +43 316 380 9835.
E-mail address: rudolf.pietschnig@uni-graz.at (R. Pietschnig).

0022-1139/$ – see front matter © 2010 Elsevier B.V. All rights reserved.
doi:10.1016/j.jfluchem.2010.07.008

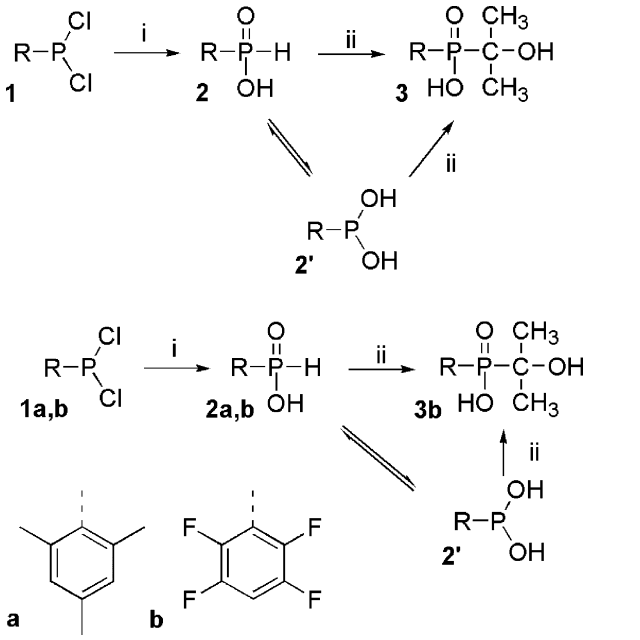

Scheme 1. Synthesis of the phosphinic acids (**2a**,**b**) and the acetone adduct (**3a**) starting from the corresponding dichlorophosphanes (**1a**,**b**). (i) H_2O, $CDCl_3$ 0 °C giving **2a** and **2b** in 99% and 75% yield, respectively. (ii) acetone (yield: 52%). For (a) R = $-C_6F_4H$ and (b) R = Mes.

trimethyl-phenyl) derivative **2b**, the electronic – unlike the steric – situation at the adjacent phosphorus atom should be very different from the fluorinated counterparts. In order to explore the balance of steric and electronic effects for these compounds we prepared **2a** and **2b** to compare their structure and reactivity.

The fluoroaryl phosphinic acid **2a** is obtained in a clean reaction by controlled hydrolysis of **1a** in chloroform solution as an oily material, which solidifies at 4 °C upon prolonged cooling after removal of the solvent in almost quantitative yields. In a similar way, the mesityl analog **2b** is obtained in 75% by a clean reaction from **1b** (Scheme 1). The IR data of solid **2a**,**b** show the presence of the P–H and the P=O functionalities [27]. For both compounds the tautomeric form present in the solid state is the phosphorane form **2** of the phosphinic acid rather than the phosphane tautomer **2′** as was clearly confirmed by X-ray diffraction on suitable single crystals.

Compound **2a** crystallizes in the monoclinic space group $P2_1/c$ as colorless plates. The phosphinic acid group in **2a** is oriented to near coplanarity of the P–H bond relative to the aryl ring (C6–C1–P1–H1 1.8(7)°) leading to a close contact with an F atom (H1···F6 2.58(2) Å). The P–H and O–H bonds are 1.28(2) Å and 0.87(3) Å, respectively, which is in the typical range for these bonds. In general phosphinic acids form strong hydrogen bonds owing to the polarity of the P–O unit. In **2a** this is further enhanced resulting in very short donor acceptor distances, which is significantly shorter than in phenyl phosphinic acid **(4)** [28], but also shorter than in [2,4,6-tris(trifluoromethyl)phenyl]-phosphinic acid **(5)** [29]. A summary of the donor acceptor geometry parameters is given in Table 1. The formation of a linear chain is typical for phosphinic acid with little steric shielding [28], while phosphinic acids with bulky substituents usually form dimers [30,31]. Short contacts of neighboring chains via the aromatic hydrogen atom exhibit weak vdW interactions H4–F2 (2.44(2) Å and H4–O1 2.70(2) Å). A graphical representation of the structure of **2a** is depicted in Fig. 1 and details of the data acquisition and structure solution are summarized in Table 2.

The mesityl substituted analog **2b** crystallizes in the monoclinic space group $P2_1/n$ as colorless needles. The phosphinic acid shows

Table 1
Geometric parameters for the donor–acceptor interactions in compounds **2a**, **2b**, **4**, **5**.

	D–H···A	D···A (Å)	D–H (Å)	H···A (Å)	D–H···A (°)
2a	O2–H2···O1	2.485(1)	0.88(3)	1.62(3)	174(3)
2b	O1–H2···O2	2.492(1)	0.83(2)	1.66(2)	172(2)
4	O2–H2···O1	2.513(3)	0.88(4)	1.64(4)	168(3)
5	O2–H2···O1	2.509(4)	0.84(5)	1.68(5)	168(5)

an orientation in a way that the P=O bond is arranged almost coplanar with the phenyl ring (O2–P1–C1–C2 10.0(1)°). The quality of the crystal of **2b** allowed the analysis of the hydrogen bond system which forms a zig-zag arranged linear chain. Also in non-fluorinated **2b** shorter donor acceptor distances than in **(4)** and **(5)** are observed which indicates that the electron withdrawing properties of the substituent in fluorinated **2a** are only in part responsible for the strong donor–acceptor interaction. Other structural parameters of **2b** show no peculiarities (Fig. 2).

To check how compounds **2a**,**b** behave in solution we performed NMR measurements in acetone. Based on ^{31}P NMR measurements the phosphinic acid R–PH(=O)OH is the only detectable tautomer for fluorinated **2a** and non-fluorinated **2b**. The chemical shifts and coupling constants are with 2.2 ppm (d, $^1J_{PH}$ = 630 Hz) (**2a**) and 24.2 (d, $^1J_{PH}$ = 562 Hz) (**2b**) in the expected range for the phosphorane form of phosphinic acids. One significant difference between **2a** and **2b** is the reaction behavior towards acetone. Unexpectedly, we found a dynamic H/D exchange for fluorinated **2a** in acetone-d^6 while no such behavior was observable for non-fluorinated **2b**. In the case of **2a** the stepwise exchange of both protons of the –PH(=O)OH functionality can be monitored with ^1H NMR where the presence of the C–H

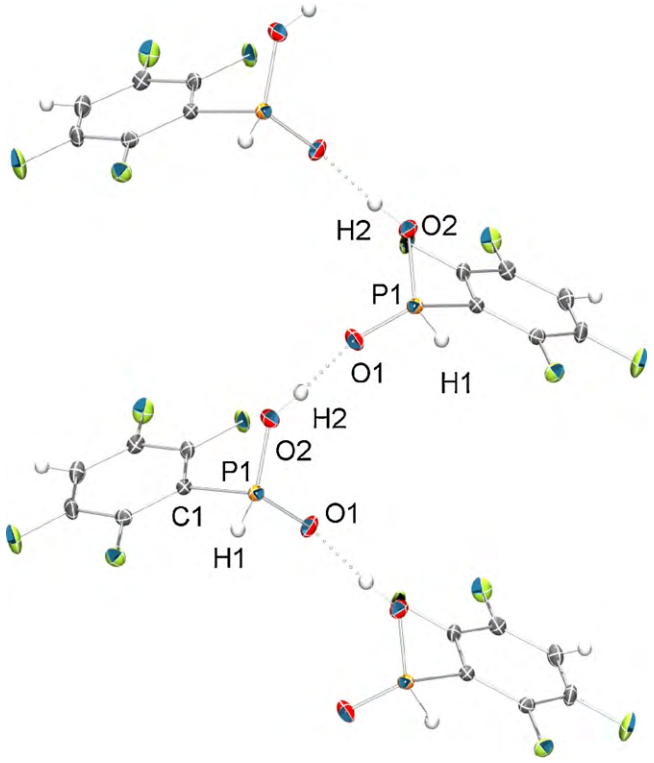

Fig. 1. ORTEP [32] drawing of the unit cell content of compound **2a** at a probability level of 50%. Compound **2a** forms an infinite chain in a zig-zag pattern along the crystallographic *c*-axis (0 0 1). Selected bond lengths (Å) and angles (°): P1–O1 1.491(1), P1–O2 1.5370(1), P1–C1 1.809(1), P1–H1 1.28(2), O2–H2 0.87(3), P1–O2–H2 119(2), O1–P1–C1–C6 121.1(1), O2–P1–C1–C6 111.5(1), C6–C1–P1–H1 1.8(7).

Table 2
Structure collection and refinement data for compounds **2a**, **2b** and **3a**. Weighting scheme $w = 1/[\sigma^2(F_o^2) + (aP)^2 + bP]$ where $P = (F_o^2 + 2F_c^2)/3$.

	2a	**2b**	**3a**
CCDC no.	753926	754559	754558
Empirical formula	$C_6H_3F_4O_2P$	$C_9H_{13}O_2P$	$C_9H_9F_4O_3P$
Formula weight	214.05	184.16	272.13
Temperature (K)	100(2)		
Wavelength (Å)	0.71073		
Crystal system	Monoclinic	Monoclinic	Monoclinic
Space group	$P2_1/c$	$P2_1/n$	$P2_1/c$
Unit cell dimensions			
a (Å)	7.8645(4)	12.6132(6)	11.8615(5)
b (Å)	13.2701(7)	5.1517(2)	18.4348(7)
c (Å)	7.1937(4)	14.6367(7)	10.5508(4)
β (°)	102.879(2)	110.060(1)	114.714(1)
Volume (Å^3)	731.87(7)	893.39(7)	2095.77(14)
Z	4	4	8
Density (calculated) (Mg/m^3)	1.943	1.369	1.725
Absorption coefficient (mm^{-1})	0.411	0.263	0.314
F(000)	1164	392	1164
Absorption correction	Semi-empirical from equivalents		
Crystal size (mm^3)	$0.38 \times 0.30 \times 0.12$	$0.66 \times 0.19 \times 0.13$	$0.20 \times 0.17 \times 0.09$
θ range for data collection (°)	2.66–30.00	1.84–30.00	1.89–30.00
Index ranges	$-9 \le h \le 11$, $-18 \le k \le 18$, $-10 \le l \le 9$	$-17 \le h \le 17$, $-7 \le k \le 7$, $-20 \le l \le 20$	$-16 < h < 16$, $-25 < k < 25$, $-14 < l < 14$
Reflections collected	8076	24158	78339
Independent reflections	2125 [R(int) = 0.0212]	2606 [R(int) = 0.0255]	6113 [R(int) = 0.0339]
Completeness to θ = 30.00° (%)	99.99	100.00	100.00
Max./min. transmission	1.000/0.834	0.9662/0.8455	0.9655/0.9253
Refinement method	Full-matrix least-squares on F^2		
Data/restraints/parameters	2125/0/130	2606/0/119	6113/0/323
Goodness-of-fit on F^2	1.066	1.004	1.046
Final R indices ($I > 2\sigma(I)$)	R1 = 0.0252, wR2 = 0.0710	R1 = 0.0297, wR2 = 0.0914	R1 = 0.0281, wR2 = 0.0798
R indices (all data)	R1 = 0.0273, wR2 = 0.0725	R1 = 0.0309, wR2 = 0.0927	R1 = 0.0349, wR2 = 0.0843
Weighting scheme parameters			
a	0.0397	0.055700	0.0437
b	0.2881	0.515700	0.8194
Largest Δ/σ in last cycle	0.000	0.000	0.000
Largest diff. peak/hole (e Å^{-3})	0.463/−0.341	0.453/−0.319	0.471/−0.312

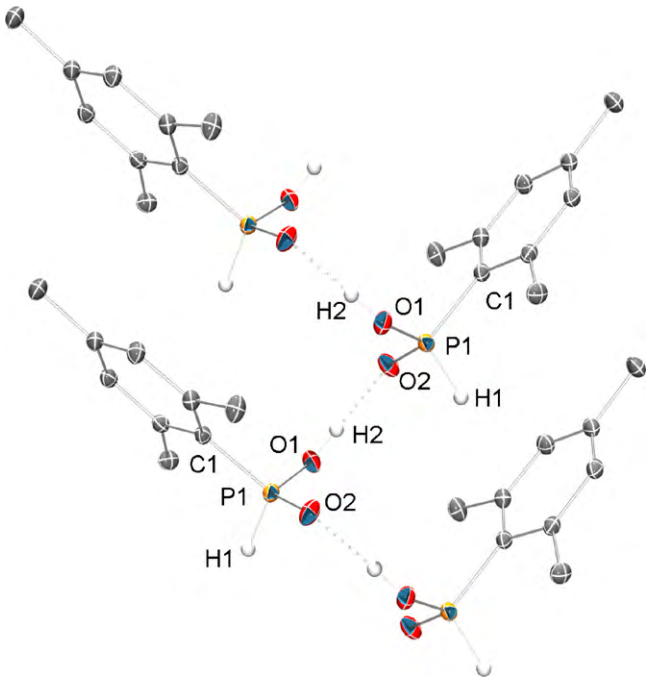

Fig. 2. Crystal structure **2b**. ORTEP [32] plot at a probability level of 50%. Hydrogen are omitted for clarity. The molecules show a zig-zag arrangement along the crystallographic b-axis (0 1 0). Selected distances (Å) and angles (°): P1–O2 1.4971(8), P1–O1 1.5531(8), P1–C1 1.802(1), P1–H1 1.35(2), O1–H2 0.83(2), P1–O1–H2 117(1), O2–P1–C1–C2 10.0(1), O1–P1–C1–C2 119.0(1).

proton turns out to be especially useful. Initially, the P–OH resonance of **2a** can be observed, but already after 5 min integrals are no longer in agreement with the intensity of the other signals (e.g. HF_4C_6–). After 12 h both proton resonances of the phosphinic acid have disappeared, owing to complete exchange with deuterium. The transfer of the more acidic OH proton to the less acidic P–H position (H/D scrambling) can be explained by a successive tautomeric equilibrium involving a sequential change of the formal oxidation state from P(V) to P(III) and vice versa as summarized in Scheme 2. As known from the literature electron withdrawing substituents favor the trivalent P(III) intermediate **2′** which explains why such an exchange is observed for **2a** but not for **2b** [8,9]. Based on DFT calculations (B3LYP/6-311G**) the preference for the phosphorane structure **2** over the phosphane structure **2′** can be quantified and as expected the energy difference is smaller for the electron-withdrawing HF_4C_6-substituent (**2′a** → **2a** $|\Delta G^{298} = -1.9$ kcal/mol and **2′b** → **2b** $|\Delta G^{298} = -6.5$ kcal/mol).

Moreover, the proton exchange is presumably facilitated via a dimeric intermediate [33]. To the best of our knowledge no evidence for P–H/P–D exchange in acetone–d^6 at ambient temperature has been reported so far. By contrast H/D exchange of primary phosphanes in D_2O is well established [34]. We assume that acetone–d^6 acts as the deuterium source owing to the α-acidity of carbonyl compounds involving the corresponding enol. The fact that H/D exchange only occurs for **2a** but not **2b** might point to the higher acidity of **2a** which may lead to protonated acetone–d^6 which then on deprotonation would be able to transfer D^+ to the conjugated base of **2a**.

In the course of the H/D exchange, the initial doublet of the ^{31}P signal of **2a** ($^1J_{PH}$ 630 Hz) turns into a triplet of constant intensity

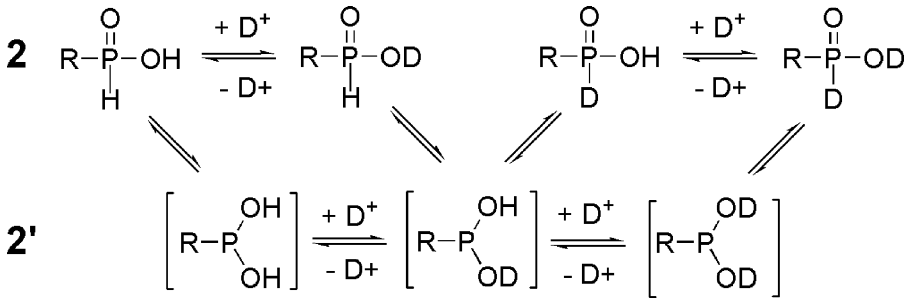

Scheme 2. Tautomeric equilibrium resulting in H/D scrambling for **2a**.

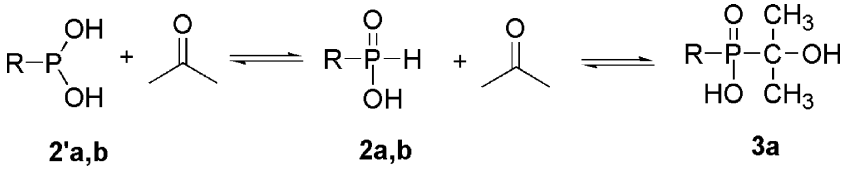

Scheme 3. Equilibrium of the free phosphinic acid **(2)** its P(III) tautomer **(2′)** and the acetone adduct **(3)** (with **a** R = 2,3,5,6-F_4C_6H– and **b** R = Mes).

due to the ^{31}P–D coupling ($^{1}J_{PD}$ 92 Hz). The ratio of the coupling constants is ~6.85, which roughly matches the ratio of the gyromagnetic constants (42.58:6.54 = 6.51). The aromatic proton in para position offers the possibility for easy detection of the aromatic carbon atom signals in HMBC ^{13}C NMR measurements and additionally the P-bonded $\underline{C}_{aryl}$ resonance (116.4 ppm) could be detected in D_2O/H_2O solution. Detection of these signals by more simple ^{13}C NMR experiments is often limited by small and broad signals owing to CF couplings over more than one bond.

In the course of the NMR measurements in acetone–d^6, we observed a broad-unresolved-signal around 46 ppm in the ^{31}P spectra, but no additional signals in the proton spectra. Hoge and co-workers described the formation of an acetone adduct of $(C_6F_5)_2P(=O)H$ in acetone in solution with a ^{31}P chemical shift at 29.2 ppm. However the latter turned out to be kinetically unstable and upon evaporation of the solvent also the incorporated acetone molecule was removed and the adduct could not be obtained and isolated in the solid state [14]. By contrast, we could easily isolate the analogous adduct **3a** in crystalline form from solutions of phosphinic acid **2a** in non-deuterated acetone, which is formed as depicted in Scheme 3. Attempts to crystallize **2a** from any other organic solvent than acetone failed however. X-ray structure analysis of these crystals confirms the presence of the phosphinic acid–acetone adduct (**3a**) in the solid state (Fig. 3). The acetone adduct was isolated in 52% yield.

Compound **3a** crystallizes in the monoclinic space group $P2_1/c$ as colorless plates. The P–C_{aryl} bond lengths are in the upper range (1.822(1) Å–1.830(1) Å) comparable to the benzaldehyde adduct of phenyl phosphinic acid (1.818(4) Å–1.821(3) Å) [20] and (2,6-$CF_3C_6H_4)_2P(=O)H$ (1.819(2) Å–1.822(2) Å) [35]. The phosphorus oxygen bonds are also in the typical range 1.482(1) Å–1.488(1) Å and 1.549(1) Å–1.554(1) Å for double and single bonds, respectively. The aliphatic hydroxyl group shows significantly shorter O–H distances (0.77(2) Å–0.81(2) Å) compared to the more acidic phosphinic OH group (0.89(2) Å–0.95(2) Å). The packing of the molecules in the solid state is dominated by the formation of a hydrogen bonded network. Compound **3a** forms an extended 2-dimensional hydrogen bonded network orthogonal to the crystallographic *b*-axis (0 1 0). Hexagonal cycles are formed by six individual molecules resulting in a honey-comb-like structure (six membered cycles *A* and *B*). Two pairs of molecules form a dimeric unit by two P=O···HO–C hydrogen bonded motifs (*C*) with O···H distances of 1.82(2) Å. These dimers are bridged by further 2 molecules via single hydrogen bonds (*D*: O···H 1.86(2) Å), *E*: O···H 1.59(2) Å). A second dimeric hydrogen bonded motif (*F*) of O···H 1.67(2) Å completes the comb like structure. Weak interactions of fluorine atoms with the phenyl rings (F6–C11 3.000(1) Å, F6–C12 2.934(1) Å, F3–C2 2.973(1) Å, F3–C3 3.155(1) Å) shows stacking between the layers formed by the H-bonded network. Relevant crystallographic details for **3a** are summarized in Table 2 and a graphical representation of the 2-dimensional network is depicted in Fig. 4.

The IR spectra of solid **3a** show a strong band 1248 cm^{-1} which can be assigned to P=O stretching modes based on calculated IR

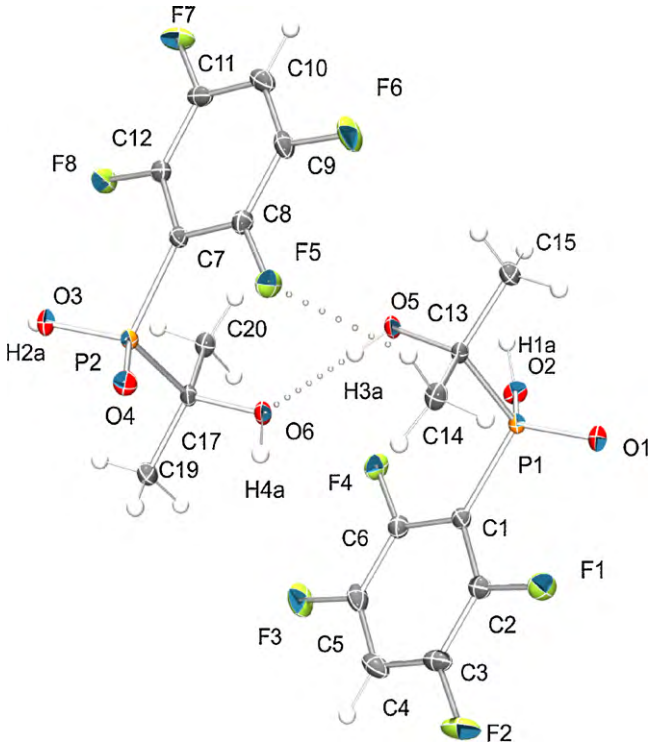

Fig. 3. ORTEP [32] drawing of **3a** at a probability level of 50%. The asymmetric unit contains two independent molecules with nearly the same geometry. Selected bond lengths (Å) and angles (°): P1–O1 1.489(1), P1–O2 1.549(1), P1–C1 1.822(1), P1–C13 1.842(1), C13–O5 1.442(1), C13–C14 1.525(1), C13–C15 1.528(1), O2–H1a 0.89(2), O5–H3a 0.78(12), O4–P2–C7–C8 33.8(1), O1–P1–C1–C2 23.5(1).

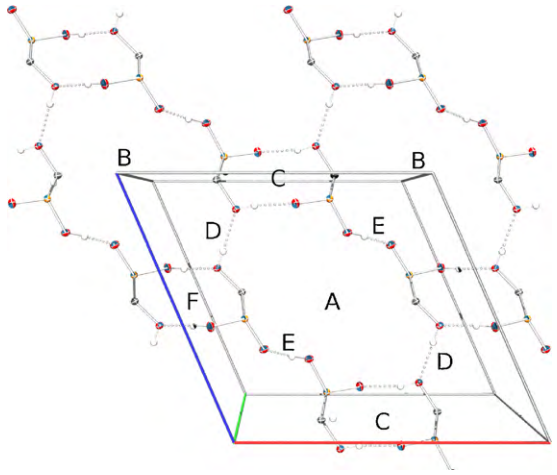

Fig. 4. View of **3a** along the *b*-axis (0 1 0) illustrating the comb like structure built of alternating hexagons A and B. HC_6F_4– and methyl-groups are omitted for clarity.

data. The strong band at around 1600 cm^{-1} can be attributed to different aromatic stretch and methyl bending modes. The different hydroxyl groups give weak broad bands around 3120 cm^{-1}. The measured bands with the exception of OH modes can be assigned reasonably based on calculated ones. The deviation for the OH vibrations may be attributed to the associated hydrogen bond network present in the experimental sample as compared to the isolated molecules in vacuo used for calculations.

A solution of crystalline **3a** in acetone–d^6 shows a singlet at 46.4 ppm in the ^{31}P NMR spectra. Furthermore, minor amounts of phosphinic acid **2a** are observed as well which is likely to be derived from elimination of acetone from **3a**. In the ^1H NMR spectra one signal for the aromatic proton (7.77 ppm) and a doublet for the methyl groups (1.39 ppm, 16.0 Hz) are observed for **3a**. According to 2D-NMR (HMBC/HSQC) measurements the proton signal of these methyl groups shows a correlation to the quaternary carbinol carbon atom ($\delta(^{13}C)$ = 70.11 ppm) which proves the connection of the methyl groups to the latter also in solution. The integrals of the proton signals of the methyl groups in **3a** are smaller than expected, which can be explained assuming a fast (on the NMR time scale) exchange of the non-deuterated acetone unit in the addition product with the deuterated acetone used as a solvent. To suspend this exchange we dissolved **3a** in tetrahydrofurane–d^8 giving a single resonance at 34.3 ppm in the ^{31}P NMR spectra, which is at rather high field compared to other α-hydroxy phosphinic acids [19]. The difference of the ^{31}P chemical shifts of **3a** in acetone and THF underlines the significance of solvent effects for this system. Similar adducts of **2a** with other ketones can be formed as well and the corresponding methylethylketone adduct shows a ^{31}P chemical shift of 38.1 ppm in chloroform solution.

An investigation of the thermodynamic balance of the adduct formation has been performed with computational methods (B3LYP/6-311G**). The surprising result is that the adduct formation of **2a** and acetone leading to **3a** is in fact an endergonic reaction (ΔG^{298} = 11.1 kcal/mol). Since the calculations refer to the gas phase, the relevant driving force for the formation of **3a** may be the formation of the extended hydrogen bonded network as found in the solid state. Nevertheless the parameters (i.e. geometry, spectroscopic data) calculated for an isolated molecule of **3a** in vacuo are in good agreement with the experimental data measured for the solid (H-bridged) compound.

3. Conclusion

In summary, we prepared a phosphinic acid with a fluorinated aryl group (**2a**) in comparison to its mesityl substituted analog (**2b**) where the steric situation is similar while the electronic situation differs. The behavior of these phosphinic acids was studied in solution indicating the exclusive presence of the phosphorane tautomer **2**, or a fast equilibrium on the NMR time scale in which the latter is dominant over the corresponding phosphane tautomer **2′**. In the solid state molecules of **2a** and **2b** are connected via their phosphorane functionalities to infinite chains via strong hydrogen bonds. Besides these similarities, their reactivity towards acetone differs substantially. A characteristic reaction of compound **2a** is the addition of the P–H unit to the carbonyl group of acetone under formation of **3a**, which occurs in solution and persists also in the solid state. Its mesityl analog **2b** does not show a reaction with acetone at all. Moreover, in solution **2a** is also involved in a dynamic proton exchange with acetone as evidenced by H/D scambling. Again its mesityl analog **2b** does not show similar behavior. According to our findings, the energetically lower accessibility of the phosphane tautomer **2′a** along with the higher acidity of **2a** are likely to be responsible for this different behavior. In summary the unique reactivity observed in the formation of **3a** allows the facile formation of a P–C bond without involvement of salt elimination or expensive or sensitive organometallic coupling reagents. An obvious perspective for future work will be the control of the reversibility of this addition also exploring the possibility to induce an enantiomeric excess for the asymmetrically substituted phosphorus center formed during this addition.

4. Supplementary information

CCDC-753926 (for **2a**), -754559 (for **2b**) and -754558 (for **3a**) contain the supplementary crystallographic data for this paper. These data can be obtained free of charge at www.ccdc.cam.ac.uk/conts/retrieving.html [or from the Cambridge Crystallographic Data Centre, 12 Union Road, Cambridge CB2 1EZ, UK; Fax: (internat.) +44 1223 336 033; E-mail: deposit@ccdc.cam. ac.uk].

For compounds **2a**,**b**, **2′a**,**b** and **3** output summaries for the DFT calculations (optimized geometries, total energies (*E*, in hartree)) have been provided as supplementary material.

5. Experimental and computational details

5.1. General

Reactions are carried out under ambient atmosphere unless otherwise noted. NMR measurements were performed on a Varian UnityInova 400 and a BrukerAvanceIII 300 operating at proton frequencies of 399.9 MHz and 300.1 MHz, respectively. ^1H and ^{13}C shifts are given in ppm and referenced to residual solvent signal. ^{19}F and ^{31}P shifts are given in ppm and are referenced externally to $C_6H_5CF_3$ (−63.7 ppm) and H_3PO_4 (85%), respectively. Dichlorophosphanes **1a**, Mes–PCl_2, and Mes–PH(=O)OH were synthesized according to published procedures [26,36,37]. Freshly bought acetone–d^6 (0.02% water) was dried over P_4O_{10} and stored in a Schlenk-tube after distillation. DFT calculations were performed with the Gaussian program package [38]. The B3LYP hybrid functional with a 6-311G** basis set was used for all calculations. All structures are fully optimized and determined to be local minima by inspection of their harmonic frequencies having no imaginary frequency. Frequencies were used without scaling factors for determination of thermal correction at 298.15 K.

5.2. Synthesis of 2a

To a solution of **1a** (240 mg, 0.96 mmol) in $CHCl_3$ (1.3 ml) ca. 2 equivalents of H_2O (40 mg, 2.2 mmol) are added. The resulting suspension is dried by slow evaporation under ambient conditions.

The phosphinic acid is insoluble in typical organic solvents, with the exception of acetone and water. Compound **2a** is an oily material which solidifies upon standing at 4 °C. Yield: 203 mg (0.95 mmol, 99%). Mp. 27 °C. ^{1}H NMR (CD_3COCD_3, 400 MHz): δ = 7.67 (1H, m, aryl), 7.90 (1H, d, $^{1}J_{PH}$ = 629.5 Hz), 8.37 (s, 1H, exchanges rapidly with acetone–d^6); ^{13}C NMR (CD_3COCD3, 100 MHz): δ = 110.61 ppm, 146.00 (dm, $^{1}J_{CF}$ 235.7 Hz), 147.53 (dm, $^{1}J_{CF}$ 259.3 Hz), $\underline{C}_{aryl}$–P 116.4 (from freshly prepared D_2O/H_2O solution). ^{31}P NMR (CD_3COCD_3, 162 MHz): δ = 2.2 ppm (d, $^{1}J_{PH}$ = 630 Hz) after 12 h. ^{1}H was completely exchanged by ^{2}H. The initial doublet becomes a triplet of constant intensity. 2.2 ppm (t, $^{1}J_{PD}$ = 92 Hz). ^{19}F NMR (THF–d^8, 282.4 MHz): δ = −141.09 (br. s, 4F). IR(KBr [cm^{-1}]): 3104 (w, $C_{arom.}$–H), 2469 (w, P–H), 2090 (m br.), 1610 (m arom.), 1484 (str, arom.), 1375 (m), 1246 (str, P=O), 863 (m, P–OH).

5.3. Synthesis of 2b

To a solution of Mes–PCl_2 (0.65 g, 2.9 mmol) in chloroform 2.5 equiv of H_2O are added at 0 °C. The mixture is stirred for 1 h. The organic phase is dried over $MgSO_4$ and the solvent removed in vacuum yielding 0.40 g pure product (2.2 mmol, 75%). Colorless crystals suitable for X-ray diffraction are obtained by slow evaporation of chloroform solutions. Mp: 143 °C. ^{1}H NMR ($CDCl_3$, 300 MHz): δ = 8.03 (1H, d, $^{1}J_{PH}$ = 562.0 Hz), 6.76 (2H, d, $^{4}J_{PH}$ 4.3 Hz, aryl), 2.57 (6H, s, *o*-CH_3), 2.28 (3H, s, *p*-CH_3). ^{13}C NMR ($CDCl_3$, 75.5 MHz): δ = 142.64 (s, C_{para}) 141.47 (d, 11.7 Hz, C_{meta}), 139.11 (d, 12.2 Hz, C_{ortho}), 124.03 (d, $^{1}J_{PC}$ 138.1 Hz, C_{ipso}), 20.96 (d, $^{3}J_{PC}$ 8.9 Hz, *m*-CH_3), 14.21 (s, *p*-CH_3). ^{31}P NMR ($CDCl_3$, 121.5 MHz): δ = 24.2 (d, $^{1}J_{PH}$ 562 Hz). IR(KBr [cm^{-1}]): 2942 (w, $C_{arom.}$–H), 2920 (w, Methyl), 2408 (w, P–H), 2155 (m. br.), 1605 (str., arom. stretch), 1561 (str., arom. stretch), 1457 (m, CH_3 bent), 1190(m, P=O stretch), 1092 (m), 964 (m), 853 (m, P–OH stretch).

5.4. Addition of 2a to acetone and formation of 3a

Phosphinic acid **2a** (174 mg, 0.81 mmol) was dissolved in acetone and placed in a screw top vial at room temperature. Small plates of **3a** suitable for X-ray diffraction were obtained after 3 weeks of crystallization. After collecting the solid material and washing with chloroform pure crystalline material was obtained. Yield 116 mg (0.43 mol, 52%). Mp. 131 °C. ^{1}H NMR (CD_3COCD_3, 400 MHz): δ = 7.77 (m, 1H, aryl), 1.39 (d, "6H", $^{3}J_{PH}$ 16.0 Hz); ^{13}C ^{1}H-HMBC/HSQC (THF–d^8, 100 MHz): 23.33 (CH_3), 70.11 (d, $^{1}J_{PC}$ 13.8 Hz), 110.76 (*p*-$C_{arom.}$), 145.02–148.61 (m, *o*- and *m*-C). $C_{arom.}$–P could not be detected. ^{31}P NMR (CD_3COCD_3, 121.5 MHz) δ = 46.4; ^{31}P NMR (THF–d^8, 121.5 MHz): δ = 34.3, ^{19}F NMR (THF–d^8, 282.4 MHz): δ = −131.64 (m, 2F, C_{ortho}–F), −141.07 (m, 2F, C_{meta}–F); IR(KBr [cm^{-1}]): 3121 br.w. 1476 (s, str), 1248 (s, str., P=O), 970 (s, m), 917 (s, m). 860 (w, P–OH).

5.5. Addition of 2a to 2-butanone

The solid phosphinic acid **2a** (27 mg, 0.13 mmol) is dissolved in 2-butanone (5 ml) and stirred at slightly elevated temperatures for 2 days. Complete conversion into the corresponding α-hydroxy phosphinic acid was checked by ^{31}P NMR spectroscopy. After removal of the excess of 2-butanone the resulting oily material is extracted with chloroform. Spectroscopically pure product is obtained as viscous oil after removal of the solvent under vacuum (33 mg, 0.12 mmol, 91%).

^{1}H NMR ($CDCl_3$, 300 MHz): δ = 0.99 (br. t, $^{3}J_{HH}$ 7.1 Hz, 3H, CH_2–$C\underline{H}_3$), 1.35 (d, $^{3}J_{PH}$ 17.2 Hz, 3H, CH_3), 1.76 (m, 2H, $C\underline{H}_2$–CH_3), 6.75 (br. S, OH), 7.26 (m, 1H, aryl). ^{13}C NMR ($CDCl_3$, 75 MHz): δ = 6.6 (CH_2–$\underline{C}H_3$), 19.2 ($\underline{C}H_2$–CH_3), 27.9 (CH_3), 73.7 (d, $^{1}J_{PC}$ 147.0 Hz, C–OH), 111.2 (C_{aryl}–H), 145.5 (dm, $^{1}J_{CF}$ 261.9 Hz, *o*, *m*-C_{aryl}), P–C_{aryl} n.d. ^{19}F NMR ($CDCl_3$, 282 MHz): δ = −128.73 (m), −136.99 (br. s). ^{31}P NMR ($CDCl_3$, 121 MHz): δ = +38.1 (br. s).

5.6. Crystallographic details

X-ray studies have been carried out with a Bruker Apex-III diffractometer equipped with a CCD detector. Structures are solved by direct methods using SHEL-XS and refined with SHEL-XL [39]. In compounds **2b** and **3a** the H atoms of the methyl groups were refined with common isotropic displacement parameters for the H atoms of the same group and idealized geometry with tetrahedral angles, enabling rotation around the X–C bond, and C–H distances of 0.98 Å. Hydrogen atoms of the phenyl rings were put at the external bisector of the C–C–C angle at a C–H distance of 0.95 Å and common isotropic displacement parameters were refined for the H atoms of the same phenyl group. All other hydrogen atoms in **2a**, **2b** and **3a** have been located on the difference Fourier map and were refined isotropically without any constraints. In Table 2, crystal and refinement data for **2a**, **2b**, and **3a** are summarized.

Acknowledgements

Financial support by the Austrian Science Fund (FWF) (Grants P18591-B03 and P20575-N19) and the EU-COST Action CM0802 "PhoSciNet" are gratefully acknowledged.

References

[1] V.S. Sergienko, G.G. Aleksandrov, Russ. J. Coord. Chem. 27 (2001) 324–340.
[2] W.W. Metcalf, W.A. van der Donk, Annu. Rev. Biochem. 78 (2009) 65–94.
[3] M. Collinsova, J. Jiracek, Curr. Med. Chem. 7 (2000) 629–647.
[4] K.B. Dillon, H.P. Goodwin, J. Organomet. Chem. 429 (1992) 169–171.
[5] M. Scholz, H.W. Roesky, D. Stalke, K. Keller, F.T. Edelmann, J. Organomet. Chem. 366 (1989) 73–85.
[6] K. Miqueu, J.-M. Sotiropoulos, G. Pfister-Guillouzo, V.L. Rudzevich, H. Gornitzka, V. Lavallo, V.D. Romanenko, Eur. J. Inorg. Chem. (2004) 2289–2300.
[7] M.L. Clarke, D. Ellis, K.L. Mason, A.G. Orpen, P.G. Pringle, R.L. Wingad, D.A. Zaher, R.T. Baker, Dalton Trans. (2005) 1294–1300.
[8] J.E. Griffiths, A.B. Burg, J. Am. Chem. Soc. 82 (1960) 1507–1508.
[9] R.C. Dobbie, B.P. Straughan, Spectrochim. Acta Part A 27 (1971) 255–260.
[10] B. Hoge, J. Bader, H. Beckers, Y.S. Kim, R. Eujen, H. Willner, N. Ignatiev, Chem. Eur. J. 15 (2009) 3567–3576.
[11] B. Hoge, B. Kurscheid, Angew. Chem. Int. Ed. 47 (2008) 6814–6816.
[12] P.A. Chase, G.C. Welch, T. Jurca, D.W. Stephan, Angew. Chem. Int. Ed. 119 (2007) 8196–8199.
[13] G.C. Welch, L. Cabrera, P.A. Chase, E. Hollink, J.D. Masuda, P. Wei, D.W. Stephan, Dalton Trans. (2007) 3407–3414.
[14] B. Hoge, S. Neufeind, S. Hettel, W. Wiebe, C. Thösen, J. Organomet. Chem. 690 (2005) 2382–2387.
[15] M. Regitz, R. Martin, Tetrahedron 41 (1985) 819–824.
[16] B. Kaboudin, N. As-habei, Tetrahedron Lett. 45 (2004) 9099–9101.
[17] B. Kaboudin, H. Haghighat, Tetrahedron Lett. 46 (2005) 7955–7957.
[18] K.L. Freeman, M.J. Gallagher, Aust. J. Chem. 19 (1966) 2025–2033.
[19] L.F. Rozhko, V.V. Ragulin, Russ. J. Gen. Chem. 74 (2004) 1087–1090.
[20] J. Cai, Z. Zhou, G. Zhao, C. Tang, Heteroatom. Chem. 14 (2003) 312–315.
[21] H. Bauer, W. Krause, P. Staniek, in: S. Clariant International Ltd. (Ed.) PCT Int. Appl. (2008).
[22] F. Ma, X. Shen, J. Ou-Yang, Z. Deng, C. Zhang, Tetrahedron: Asymmetry 19 (2008) 31–37.
[23] M. Drag, R. Grzywa, J. Oleksyszyn, Bioorg. Med. Chem. Lett. 17 (2007) 1516–1519.
[24] M. Schlosser, D. Michel, Tetrahedron 52 (1996) 99–108.
[25] A. Bondi, J. Phys. Chem. 68 (1964) 441–451.
[26] A. Orthaber, F. Belaj, R. Pietschnig, J. Organomet. Chem. 695 (2010) 974–980.
[27] By comparison of the calculated with the measured IR spectra bands at 2469 (2503) and 1246 (1273) for **2a** and 2408 (2424) and 1190 (1244) are assigned to P–H and P=O stretching modes, respectively. Measured (calculated) wavenumbers [cm^{-1}].
[28] R.A. Burrow, D.H. Farrar, A.J. Lough, M.R. Siqueira, F. Squizani, Acta Crystallogr. Sect. C: Cryst. Struct. Commun. 56 (2000) e357–e358.
[29] S.M. Cornet, K.B. Dillon, J.A.K. Howard, P.K. Monks, A.L. Thompson, Acta Crystallogr. Sect. C: Cryst. Struct. Commun. 65 (2009) o195–o197.
[30] Y. Belabassi, A.F. Gushwa, A.F. Richards, J.-L. Montchamp, Phosphorus Sulfur Silicon Relat. Elem. 183 (2008) 2214–2228.
[31] C. Nolde, M. Schürmann, M. Mehring, Z. Anorg. Allg. Chem. 633 (2007) 142–150.
[32] L.J. Farrugia, J. Appl. Crystallogr. 30 (1997) 565.
[33] N.S. Golubev, R.E. Asfin, S.N. Smirnov, P.M. Tolstoi, Russ. J. Gen. Chem. 76 (2006) 915–924.
[34] B.-M. Fung, I.Y. Wei, J. Am. Chem. Soc. 92 (1970) 1497–1501.

[35] B. Hoge, B. Kurscheid, S. Peuker, W. Tyrra, H.T.M. Fischer, Z. Anorg. Allg. Chem. 633 (2007) 1679–1685.
[36] J.F. Brazier, F. Mathis, R. Wolf, C. R. Chim. 262 (1966) 1393–1396.
[37] H. Goldwhite, J. Kaminski, G. Millhauser, J. Ortiz, M. Vargas, L. Vertal, M.F. Lappert, S.J. Smith, J. Organomet. Chem. 310 (1986) 21–25.
[38] M.J. Frisch, G.W. Trucks, H.B. Schlegel, G.E. Scuseria, M.A. Robb, J.R. Cheeseman, J.A. Montgomery Jr, T. Vreven, K.N. Kudin, J.C. Burant, J.M. Millam, S.S. Iyengar, J. Tomasi, V. Barone, B. Mennucci, M. Cossi, G. Scalmani, N. Rega, G.A. Petersson, H. Nakatsuji, M. Hada, M. Ehara, K. Toyota, R. Fukuda, J. Hasegawa, M. Ishida, T. Nakajima, Y. Honda, O. Kitao, H. Nakai, M. Klene, X. Li, J.E. Knox, H.P. Hratchian, J.B. Cross, C. Adamo, J. Jaramillo, R. Gomperts, R.E. Stratmann, O. Yazyev, A.J. Austin, R. Cammi, C. Pomelli, J.W. Ochterski, P.Y. Ayala, K. Morokuma, G.A. Voth, P. Salvador, J.J. Dannenberg, V.G. Zakrzewski, S. Dapprich, A.D. Daniels, M.C. Strain, O. Farkas, D.K. Malick, A.D. Rabuck, K. Raghavachari, J.B. Foresman, J.V. Ortiz, Q. Cui, A.G. Baboul, S. Clifford, J. Cioslowski, B.B. Stefanov, G. Liu, A. Liashenko, P. Piskorz, I. Komaromi, R.L. Martin, D.J. Fox, T. Keith, M.A. Al-Laham, C.Y. Peng, A. Nanayakkara, M. Challacombe, P.M.W. Gill, B. Johnson, W. Chen, M.W. Wong, C. Gonzalez, J.A. Pople, in: Gaussian Inc., Pittsburgh, PA, 2003.
[39] G. Sheldrick, Acta Crystallogr. Sect. A: Found. Crystallogr. A64 (2008) 112–122.